Dissipative Orbiting in ^{209}Bi + ^{136}Xe Collisions at $E_{lab}/A = 28$ MeV

S. P. Baldwin, B. Lott,* B. M. Szabo, B. M. Quednau,* W. U. Schröder, and J. Tõke
Department of Chemistry and Nuclear Structure Research Laboratory, University of Rochester, Rochester, New York 14627

L. G. Sobotka, J. Barreto,† R. J. Charity, L. Gallamore,‡ D. G. Sarantites, and D. W. Stracener§
Department of Chemistry, Washington University, St. Louis, Missouri 63130

R. T. de Souza‖
Department of Physics and National Superconducting Cyclotron Laboratory, Michigan State University, East Lansing, Michigan 48824
(Received 16 June 1994)

Massive, projectilelike fragments (PLF) from the ^{209}Bi + ^{136}Xe reaction at $E_{lab}/A = 28$ MeV were measured in coincidence with lighter charged products and neutrons, detected with 4π angular coverage. Strong correlations are observed between the deflection angle of the massive fragment, on the one hand, and various experimental measures of energy dissipation, on the other hand. These correlations, as well as the observed broadening of the primary PLF atomic-number distribution with increasing energy dissipation, are strikingly reminiscent of damped reaction features that are well understood in terms of dissipative orbiting.

PACS numbers: 25.70.Lm

In recent years, the main thrust of heavy-ion reaction studies at bombarding energies per nucleon comparable to the nucleonic Fermi energy was aimed at demonstrating the occurrence of phenomena not encountered at lower bombarding energies, such as, for example, multifragmentation or vaporization [1–5]. Relatively little effort has been spent to explore systematically the transitional features of heavy-ion collision dynamics developing from the well-known damped or dissipative reaction mechanism [6], dominating at bombarding energies of only a few MeV per nucleon above the interaction barrier. Very recently, however, it has been demonstrated [7–9] in studies of the ^{209}Bi + ^{136}Xe and ^{197}Au + ^{208}Xe reactions that for these massive systems, at the lower boundary of the Fermi energy domain, the total reaction cross section is still almost entirely accounted for by binary collisions, in which, with some allowance for emission of light particles, two and only two fragments emerge initially from the collision site. The present Letter focuses on selected dissipative features of the projectilelike fragment (PLF) yield discovered in the ^{209}Bi + ^{136}Xe experiment of Ref. [7] and reported previously in several preliminary accounts [10]. Observations of the persistence of dissipative dynamics at intermediate bombarding energies have also been reported in other works [9,11].

The experiment was performed at the National Superconducting Cyclotron Laboratory of Michigan State University. A beam of 28 MeV/nucleon ^{136}Xe ions from the K1200 cyclotron was focused on a self-supporting, 1.5 mg/cm^2 thick ^{209}Bi target. The detector setup provided a virtually 4π angular coverage for neutrons, as well as for light and intermediate-mass charged reaction products. Massive fragments were measured using two position-sensitive and one "plane" multielement silicon detector telescopes. The former two covered angular ranges from 3.0° to 5.6° and 11.5° to 15.1°, respectively, while the latter telescope covered a range from 23.1° to 27.9°. The present work discusses in detail only data obtained with the most forward telescope; the others were used only in cross section estimates. This small-angle "master" telescope provided atomic-number identification for charged products with $2 \leq Z \leq 54$ and kinetic energies per nucleon of $E/A > 6$ MeV. Neutrons were detected using the Rochester RedBall neutron multiplicity meter [12], which, in this application, had an overall neutron detection efficiency of $\epsilon \approx 50\%$ for all neutrons emitted in the reaction, with a significantly higher sensitivity ($\epsilon \approx 70\%$) to neutrons emitted from slow-moving sources. Light charged products and intermediate-mass fragments (IMF) were detected using the Washington University Dwarf array [13], covering a solid angle of about 80% of 4π. A more detailed description of the setup is given elsewhere [12].

Experimental results are shown in Figs. 1–4. Figure 1 depicts a two-dimensional contour diagram of the yield, plotted vs energy (E) and atomic number (Z) of charged reaction products observed within the angular range of 3°–5.6°. As seen in this figure, the charged-product yield is concentrated in a well-defined ridge connecting, in a continuous fashion, the region of quasielastic events, at $Z \approx 54$ and $E \approx 3.8$ GeV, with that of the intermediate-mass fragments near the origin of the plot. It is worth noting that the above ridge is free of contamination by fragments from either fission of the targetlike fragments (TLF), or from symmetric PLF fission. The former have too little energy to overcome the Z-identification threshold of the telescope, while the absence of the latter fragments is evidenced by the lack of a bimodal yield pattern [8]

0031-9007/95/74(8)/1299(4)$06.00

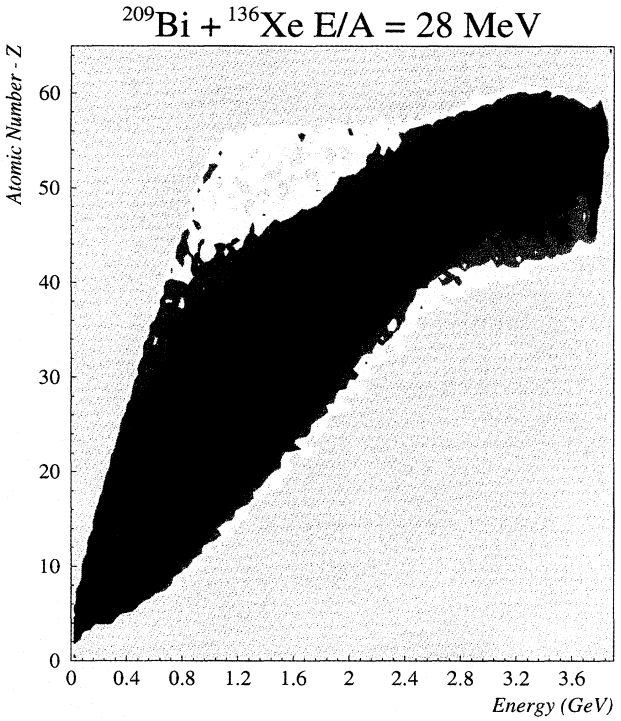

FIG. 1. Contour diagram of the yield of charged reaction products from the ^{209}Bi + ^{136}Xe reaction observed in an angular range of 3°–5.6°, plotted versus kinetic energy and atomic number of the product.

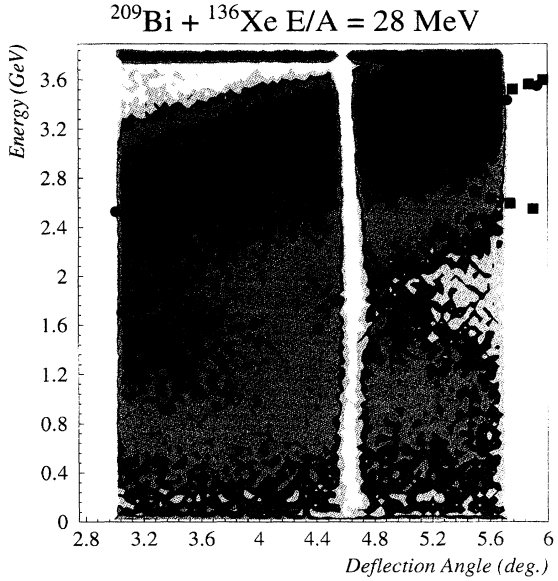

FIG. 2. Same as Fig. 1, except plotted versus deflection angle and kinetic energy of the product. Solid circles and squares represent results of calculations based on the nucleon exchange model with standard and hard-core interaction potentials, respectively.

(two kinematical solutions) in Fig. 1, characteristic of PLF fission. Asymmetric PLF fission is indistinguishable from IMF emission and can sufficiently accurately be identified based on the value of the atomic number of the fragment.

Figure 2 shows correlations between laboratory kinetic energy and emission angle for the charged reaction products, in the form of a two-dimensional contour diagram. In this representation, most of the yield of the massive fragments is seen to be distributed along two well-defined ridges. One of these ridges extends, with decreasing intensity, from the region of quasielastic yield around the grazing angle ($\Theta_{lab} \approx 7°$) toward lower energies and smaller angles. The second ridge shows the opposite trend with deflection angle, for both intensity and energy. The distribution of yield in Fig. 2 strongly suggests that the two ridges seen are actually two sections of one continuous ridge, the missing portion of the ridge falling outside the angular aperture of the master telescope. The correlations seen in Fig. 2 are reminiscent of the well-known Wilczyński plots illustrating the deflection function for binary heavy-ion collisions at energies of a few MeV/nucleon above the interaction barrier.

Experimental data are compared in Fig. 2 with the predictions of dynamical model calculations [14] based on stochastic nucleon exchange model (NEM) [15], using either the standard liquid-drop interaction potential with proximity corrections (solid circles) or the frozen-density proximity potential featuring a repulsive core (solid squares). In each case, the code EVAP [16] was used to simulate the decay of the excited primary reaction products. Both calculations underpredict significantly the yield in the upper section of the ridge ($\sigma_u^{NEM} \approx 2$ b) and attribute too much cross section ($\sigma_l^{NEM} \approx 4$ b) to the lower branch or to fusion. For example, with $\sigma_{fus}^{NEM} \approx 1.5$ b, the standard NEM calculation overestimates the fusion cross section, which experimentally is compatible with zero. Calculations were also performed with the Boltzmann-Uehling-Uhlenbeck (BUU) model [17], for a "stiff" ($K = 380$ MeV) and a "soft" ($K = 200$ MeV) equation of state, which both lead to deflection functions indicating much stronger orbiting than observed experimentally, corresponding to $\sigma_l^{BUU} \approx 2.2$ b and $\sigma_l^{BUU} \approx 1.8$ b, respectively. Thus, neither NEM nor BUU calculations reproduce the magnitudes of the cross sections of upper and lower branches separately.

Integration of the yield of fragments with $Z \geq 20$ in any of the three telescopes results in an observed cross section of $\sigma = 3.0$ b (fragments with $Z < 20$ are mostly IMF's and were excluded to avoid double counting). Exponential interpolation of the angular distribution of the fragments, in the angular ranges between the observed sections of the ridge, results in a reaction cross section of approximately $\sigma = 5.1$ b, with an uncertainty estimated

at 15%. Note that here the angular range between 5.6° and the grazing angle is excluded. In the same angular range, classical trajectory calculations performed with the code CLAT [14] result in a cross section (fusion included) of 5.0 b. The fact that the latter number almost coincides with the 5.1 b, found here for binary processes, is consistent with the findings [7–9] that, in this bombarding energy and mass domain, almost the entire reaction cross section is accounted for by a binary primary collision scenario. The same model calculations predict 6.3 b for the total reaction cross section.

A further demonstration of the resemblance between the phenomenology of the present reaction and that of damped reactions at lower energies is given in Fig. 3. In this figure, the primary PLF atomic-number (Z_{prim}) distributions are plotted as functions of the degree of energy dissipation, expressed in terms of the measured neutron multiplicity. The primary atomic numbers were deduced by adding to the measured secondary atomic numbers (Z) the charge (ΔZ) evaporated from the PLF's, as derived from the invariant emission patterns measured with the Dwarf array. As seen from this figure, the primary atomic-number distributions broaden with increasing energy dissipation, while their averages show only a weak drift away from the projectile Z. The observed trends in the primary atomic-number distributions are quantitatively compatible with predictions of dynamical NEM calculations described above.

From Figs. 2 and 3, a reaction scenario similar to that of damped collisions can be inferred. In this scenario, the two reaction partners form a transient dinuclear system and orbit about each other for a fraction of a revolution, while relative kinetic energy is dissipated through incoherent multinucleon exchange. This is a process termed here "dissipative orbiting," regardless of the magnitude of the "orbiting angle" and, hence, of the sign of the asymptotic emission angle. Eventually, due to the repulsive Coulomb and centrifugal forces, the orbiting complex reseparates into two excited fragments, which subsequently decay statistically, predominantly via emission of light particles, but often also via fission. The dynamical reseparation into two and only two products defines the present use of the term "binary," as an attribute of the primary collision phenomenology, and not of the final count of reaction products in the exit channel.

For a further understanding of the dynamics governed by the l-dependent macroscopic interaction forces, it is interesting to explore whether the lower section of the ridge in Fig. 2 represents negative or positive deflection angles and, hence, whether a rainbow phenomenon occurs in a relatively narrow angular range along the orbiting ridge, falling outside the acceptance angle of the telescope.

The question of a possible rainbow is addressed schematically in Fig. 4, where the average emission angle (Θ_{lab}) of the massive residue of the primary PLF is plotted versus the average multiplicity of associated p, d, and t particles, along the orbiting ridge. The vertical bars illustrate the widths (FWHM) of the respective multiplicity distributions. In order to help visualize the two possible signs of the associated deflection angles, the data corresponding to the lower section of the ridge in Fig. 2 are plotted at both negative and positive angles. First, Fig. 4 confirms, in a direct fashion, a steady increase in energy dissipation, as one moves along the upper section of the ridge, from the quasielastic region toward smaller angles, and then continues along the lower section toward larger angles. Figure 4 shows also that an "S"-shape connecting section (dot-dashed line) of the ridge is needed

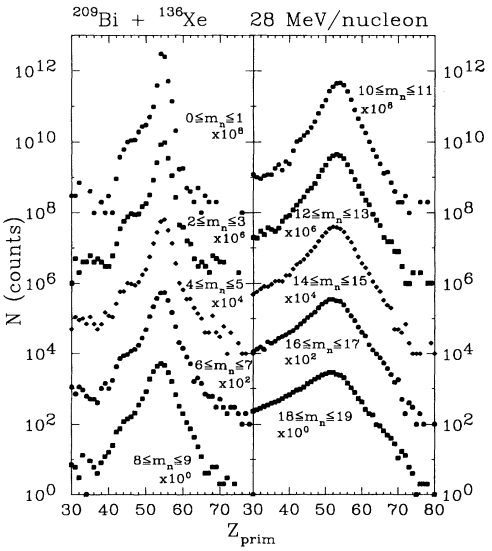

FIG. 3. Distributions of primary atomic numbers (Z_{prim}) of the projectilelike fragments for different bins in associated neutron multiplicity, as indicated.

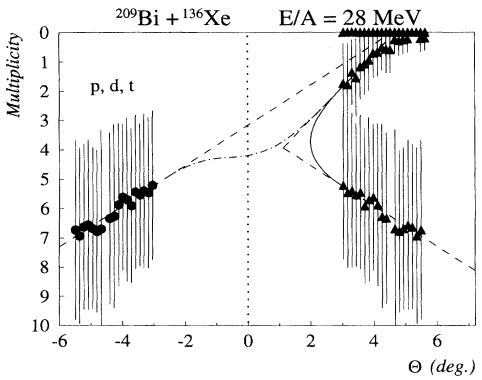

FIG. 4. Analysis of the yield ridge line in a representation of deflection angle versus measured average multiplicity of light charged particles. The lower yield branch has been plotted both at positive and at negative angles. The vertical bars illustrate FWHM values of the respective multiplicity distributions. The various curves represent different extrapolations of the two branches of measured yield discussed in the text.

to accommodate negative deflection angles for the lower section of the ridge. Similar S-shape connecting sections were found necessary for continuity in the correlation between PLF deflection angle and several other observables, including (i) PLF kinetic energy, (ii) PLF atomic-number, multiplicities of (iii) protons, (iv) deuterons, (v) tritons, and (vi) α particles. To our knowledge, an S turn has never been observed in experimental deflection functions; it would imply nonmonotonic variations with l of the effective interaction forces. On the other hand, a simple V turn (solid line) suffices to connect the two sections, were they both at positive deflection angles, and this type of turn provides no unusual theoretical challenge. Although the simple geometrical analysis of Fig. 4 is not conclusive, it provides reasonable grounds for a cautious supposition that the lower section of the ridge actually represents positive deflection angles and, hence, that a rainbow phenomenon occurs in these collisions at an angle around 2°. If confirmed, this conclusion would contradict the above standard BUU and NEM calculations, which do not show such a rainbow feature at positive deflection angles.

In summary, two sections of the deflection function have been observed for the ^{209}Bi + ^{136}Xe reaction at E/A = 28 MeV and an angular range of 3°–5.6°, corresponding to two different ranges of kinetic-energy dissipation and associated impact parameter. The observed evolution of the primary PLF atomic-number (Z_{prim}) distributions with the degree of energy damping points to an underlying collision scenario similar to that encountered in damped reactions at lower bombarding energies. From simple geometrical considerations, it can be argued that possibly both observed branches of the deflection function correspond to positive deflection angles, indicative of the nuclear rainbow phenomenon. Neither, the dynamical one-body exchange model nor the BUU approach, in their current implementations, account quantitatively for the macroscopic reaction dynamics. Clearly, more systematic studies, spanning a range of systems and bombarding energies, are needed to provide directions for a further development of a quantitative theory of macroscopic nuclear interactions in the Fermi energy domain.

We would like to thank Professor W. Bauer for providing his well-documented BUU code for our use. This work was supported by the U.S. Department of Energy Grants No. DE-FG02-88ER40414 (University of Rochester), No. DE-FG02-87ER403160 and No. DE-FG02-88ER40406 (Washington University), and by National Science Foundation Grant No. PHY-89-13815 (NSCL).

*Presently at GANIL, B.P. 5027, F-14021 Caen, France.
†Presently at Instituto de Fisica da UFRJ, Rio de Janeiro, Brazil.
‡Presently at International Technologies, Earth City, Missouri.
§Presently at Oak Ridge National Laboratory, Oak Ridge, TN 37830.
‖Presently at Indiana University, Department of Chemistry, Bloomington, IN 42405.

[1] G.F. Bertsch and S. Das Gupta, Phys. Rep. **160**, 189 (1988), and references therein.
[2] J.P. Bondorf *et al.*, Nucl. Phys. **A443**, 321 (1985); **A444**, 460 (1985).
[3] J.A. Lopez and J. Randrup, Nucl. Phys. **A503**, 183 (1989); **A512**, 345 (1990).
[4] D.H.E. Gross, Prog. Part. Nucl. Phys. **30**, 155 (1993), and references therein.
[5] L.G. Moretto and G.J. Wozniak, Annu. Rev. Nucl. Part. Sci. **43**, 379 (1993).
[6] W.U. Schröder and J.R. Huizenga, in *Treatise in Heavy-Ion Science,* edited by D.A. Bromley (Plenum Press, New York and London, 1984), Vol. 2, p. 113, and references therein.
[7] B. Lott *et al.*, Phys. Rev. Lett. **68**, 3141 (1992).
[8] B.M. Quednau *et al.*, Phys. Lett. B **309**, 10 (1993).
[9] J.F. LeColley *et al.*, Phys. Lett. B **325**, 317 (1994).
[10] S.P. Baldwin *et al.*, in *Proceedings of the 9th Workshop on Nuclear Dynamics,* edited by B. Back *et al.* (World Scientific, Singapore, 1993), p. 36; W.U. Schröder, in *International Seminar-School on Heavy-Ion Physics, Dubna, 1993,* edited by Yu. Ts. Oganessian *et al.*, Vol. 2, p. 166.
[11] R.J. Charity *et al.*, Z. Phys. A **341**, 53 (1991).
[12] S.P. Baldwin, Ph.D. thesis, University of Rochester, 1994; Nucl. Phys. **A341**, 53 (1991).
[13] D.W. Stracener *et al.*, Nucl. Instrum. Methods Phys. Res., Sect. A **294**, 485 (1990).
[14] W.U. Schröder *et al.*, Nucl. Sci. Res. Conf. Ser. **11**, 255 (1987).
[15] J. Randrup, Nucl. Phys. **A307**, 319 (1978); **A327**, 490 (1979); **A383**, 468 (1982).
[16] N.G. Nicolis, D.G. Sarantites, and J.R. Beene, computer code EVAP (unpublished); evolved from code PACE by A. Gavron, Phys. Rev. C **21**, 230 (1980).
[17] W. Bauer, Prog. Part. Nucl. Phys. **30**, 45 (1993).

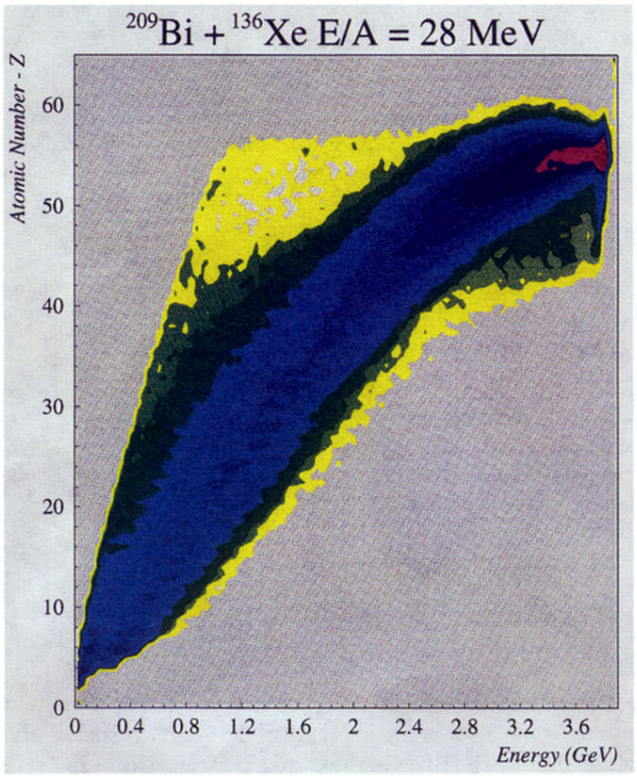

FIG. 1. Contour diagram of the yield of charged reaction products from the ^{209}Bi + ^{136}Xe reaction observed in an angular range of 3°–5.6°, plotted versus kinetic energy and atomic number of the product.

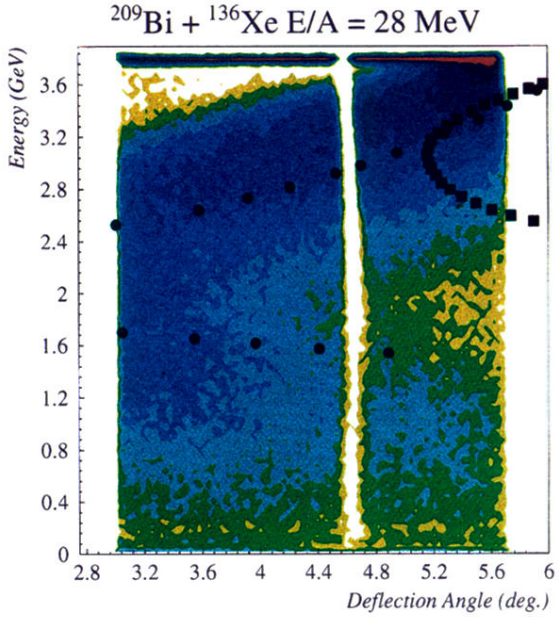

FIG. 2. Same as Fig. 1, except plotted versus deflection angle and kinetic energy of the product. Solid circles and squares represent results of calculations based on the nucleon exchange model with standard and hard-core interaction potentials, respectively.